THEORETICAL AND EXPERIMENTAL STUDY ON FULLY-DEVELOPED COMPARTMENT FIRES

Y. Utiskul[1] and J. G. Quintiere[2]
[1] ArupFire, Arup North America Ltd, Los Angeles, California 90066, USA
[2] Department of Fire Protection Engineering, University of Maryland, College Park Maryland 20742, USA

ABSTRACT

Fuel responses to the flame and its surroundings are essential to predict the effect of fire on the structures. This study explores these effects and applies them to the common fuel configurations. The study focuses on the fully-developed fires where all available fuel becomes involved and can potentially yield the severest damage to the structural elements. A single-zone fire model is developed along with a fuel mass loss rate model that accounts for the thermal enhancement, oxygen-limiting feedback, and the fuel configuration. An empirical correlation for mixing of oxygen into the lower floor layer essential for the modeling is developed. An experimental program for single-wall-vent compartment using wood crib and heptane pool is performed to validate the model and explore a full range of phenomena associated with fully-developed fires. The simulation from the model is able to capture these phenomena and shows good agreement with the experiments. Some generalities of the fuel mass loss rate and compartment gas temperature are presented using the experimental results and the model simulations. The developed model has a potential to give burning time and temperature in a fire for any fuel, scale and ventilation.

KEYWORDS: Compartment Fire, Fully-Developed, Vent Mixing, Single Zone Model, Fuel response

INTRODUCTION

A *fully-developed fire* is defined as the stage of fire where all available fuels become involved and the fire burns at its maximum potential according to the limit amount of the available fuel (*fuel-controlled fire*) or the available air supply (*ventilation-controlled fire*). At this stage, the heat flux conditions in the room can reach as high as 150 kW/m^2 [1] and a gas temperature can achieved in the range of 700 to 1200 ºC[2] which can possibly cause severe damage to the structure. Hence, the fully-developed stage is the greatest concern to the design for the structural stability and the safety of the firefighters.

In most buildings, fires in common residential spaces and offices become ventilation-controlled when the fully-developed stage is reached. In ventilation-controlled fires, all of available fuel gases are not consumed by the flames and these gases can burn as they pass through the openings causing the flames to emerge windows and doors. For a large fire at the fully-developed stage, the compartment is often filled with the smoke and the layer interface is close to the floor. Such a condition can be termed the *well-mixed* stage where the gas is assumed to have uniform properties throughout the compartment. A *single-zone* model assumption is usually suitable for this type of fires.

In a structural fire protection design, the information of the maximum temperature and fire duration is necessary to obtain a proper fire protection system for a given room with ventilation and fuel load configurations. To achieve such a requirement the *burning rate* and the *fuel mass loss rate* must be correctly calculated by taking into account for the fuel response to the thermal feedback enhancement from the enclosure and the vitiated oxygen effects. Current design tools including correlations and mathematical fire models do not address the fuel response; hence the burning time and temperature may not be properly predicted.

This paper presents a study that may fulfill the incompleteness of the current design tools by establishing a single-zone fire model that addresses the fuel response to the thermal feedback and limited oxygen effect and potentially gives the burning time and temperature for any fuel, scale, and ventilation.

COMPARTMENT BURNING RATE AND FUEL BEHAVIOR

The burning rate is defined as the rate at which the fuel, usually but not exclusively in the gas-phase, is consumed by the chemical reaction within the enclosure. The burning rate plays a significant role in compartment fire because it represents how much energy is released into the system. The energy release rate or fire power, $\dot{Q}$, within the enclosure is given as:

$$\dot{Q} = \Delta h_c \dot{m}_b \quad [1]$$

where $\dot{m}_b$ is the burning rate and Δh_c is the heat of combustion per unit mass of fuel. In some literature, however, the term burning rate was used to describe the fuel mass loss rate. While these two rates may arguably follow the same trend; they have completely different meaning. The fuel mass loss rate refers to the rate at which a condensed-phase fuel is decomposed to gases due to the energy transferred from its surrounding heat sources such as flames, hot gas, and enclosure walls. We can describe the relationship for the mass loss rate and the burning rate as follows:

$$\dot{m}_b = \begin{cases} \dot{m}_F & ;\phi < 1 \\ \dot{m}_o / s & ;\phi \geq 1 \end{cases} \quad [2]$$

where $\dot{m}_o$ is the incoming air flow rate, $\dot{m}_F$ is the fuel mass loss rate, s is the stoichiometric mass of air to fuel ratio and the global equivalence ratio $\phi = \dot{m}_F / \dot{m}_o \cdot s$. In compartment fire experiments the fuel mass loss rate can be directly measured using weighing cells to track the weight of the fuel over time; however, measurement for the burning rate may not be done directly especially in the under-ventilated condition. In order to predict the burning rate, the fuel mass loss rate must be accurately known as appears in Eq. [2]. This is always true even for the under-ventilated condition, where burning depends on available air, because the fuel mass loss rate also determines the burning state. The fuel mass loss rate can be given as [3]:

$$\dot{m}_F = \dot{m}''_{F,o} A_{F,b} \frac{Y_{ox,l}}{Y_{ox,o}} + \frac{\dot{q}_{External}}{L} \quad [3]$$

where $\dot{m}''_{F,o}$ is the free burning rate or fuel mass loss rate in opened environment per unit area, $A_{F,b}$ is the burning fuel exposed area, $Y_{ox,l}$ is the oxygen mass fraction feeding the flame, $Y_{ox,o}$ is the oxygen fraction in the free burning generally equals to 0.233, L is the heat of gasification depending on the fuel type, and $\dot{q}_{External}$ is the total external heat feedback from smoke and compartment wall surfaces. The first term on the right hand side of Eq. [3] represents the *vitiated oxygen effect* on the flame heat flux [4,5] and the second term is responsible for the *thermal feedback* from smoke and compartment wall surfaces.

A common correlation for the free burning rate per unit area of large liquid pool fires ($D > 0.2$ m) is given as [6] $\dot{m}''_{F,o} = \dot{m}''_{F,\max}\left(1 - e^{-\kappa_f L_f}\right)$, where $\dot{m}''_{F,\max}$ is the asymptotic value for fuel mass loss rate, κ_f is the flame absorption coefficient depending on the fuel type, and L_f is the mean beam length. For a cylindrical shape flame with a diameter (D), $L_f = 0.66D$ [2]. A correlation describing the time-average

free burning rate per unit exposed area for wood cribs, A_F , was established by Heskestad[7] as $\dot{m}''_{F,o} = 0.968 C_w b^{-1/2} \left(1 - \exp\left(-(sb)^{1/2} A_{C,o} / 0.02 A_F\right)\right)$, where b is the thickness dimension of a stick, s is the spacing between sticks, $A_{C,o}$ is the cross-sectional area of the vertical crib shafts, and C_w is the empirical wood crib coefficient given by Block [8].

The total external radiation feedback can be given as $\dot{q}_{External} = \dot{q}_{Ext,b} + \dot{q}_{Ext}$, where $\dot{q}_{Ext,b}$ and $\dot{q}_{Ext}$ are the net radiation feedback to the flaming fuel area and non-flaming fuel area respectively and can be given as follows:

$$\begin{aligned} \dot{q}_{Ext,b} &= F_g \left(1-\varepsilon_f\right)\varepsilon_g A_{Fp,b}\left(T^4 - T_o^4\right) + F_w \left(1-\varepsilon_f\right)\left(1-\varepsilon_g\right) A_{Fp,b}\left(T_w^4 - T_o^4\right) \\ \dot{q}_{Ext} &= F_g \varepsilon_g \left(A_{Fp} - A_{Fp,b}\right)\left(T^4 - T_v^4\right) + F_w \left(1-\varepsilon_g\right)\left(A_{Fp} - A_{Fp,b}\right)\left(T_w^4 - T_v^4\right) \end{aligned} \qquad [4]$$

where T is the compartment gas temperature, T_o is the ambient temperature, T_w is the wall temperature, T_v is the fuel vaporization temperature or the fuel surface temperature, F_g is the shape factor from the fuel to the compartment gas, F_w is the shape factor from the fuel to the walls, $A_{Fp,b}$ is the projected flaming fuel surface area, and A_{Fp} is the total projected fuel surface area, ε_f and ε_g are the emissivity of the flame and the smoke respectively.

NEAR VENT MIXING

To predict the fuel mass loss rate, the concentration of the oxygen feeding the flame, $Y_{ox,l}$, needs to be estimated. In room fires when the vent is small and the smoke layer descends close to the floor, the entering cold fresh air stream can be contaminated by the smoke due to the buoyancy and shear mixing [9] occurring near the vent. This phenomenon, called vent mixing, leads to the reduction in oxygen feeding the flame and it is therefore an important factor to explain the effect of ventilation on the fuel mass loss rate in the compartment fires. A method of characterizing the near vent mixing behavior has not been well established; however, some investigations have been carried out. Quintiere et al. [10] showed a visualization for mixing near a vent using a smoke trace technique. They also observed in their experiment mixing occurred as the cold air jet entered the doorway, expanded horizontally and descended towards the floor. McCaffrey and Quintiere [11] suggested that the flow rate of the mixed stream can be significant relative to the vent flow rate. Zukoski et al. [12, 13] developed a correlation for the mixing rate from saltwater simulation experiments. Zukoski's correlation was based on an assumption that the cold incoming flow through the opening would behave like a point source buoyant plume entraining the hot gas in the upper layer and then descending downward to the lower layer. However, Zukoski pointed out for the point source plume approach that it was illogical for two reasons. First, the plume theory was developed to describe the far field of a weakly buoyant, axisymmetric plume while the doorway plume is not axisymmetric. Secondly, the doorway incoming flow has initial momentum which is not always negligible. In this study, the mixing model was investigated based on Quintiere and McCaffrey [14] that the incoming cold air behaved like a jet entering the doorway with a characteristic velocity and diffusing downward because of buoyancy. While the cold air descended, the surrounding hot gas was entrained with a velocity that is proportional to the incoming flow characteristic velocity. From this concept, we obtain a ratio of mass entrained to the total incoming mass flow rate or mixing ratio as:

$$\frac{\dot{m}_e}{\dot{m}_o} \sim \left(\frac{T_o}{T}\right)\left(1 + \frac{N-S}{W_o}\right)\left(\frac{N-Z}{N-S}\right) \qquad [5]$$

where $\dot{m}_e$ is the mixing rate, W_o is the opening width, *S* is the sill height, *Z* is the smoke layer height, and *N* is the neutral plane height. Hence, we wish to obtain a correlation for the mixing ratio empirically in the form of Eq. [5]. Single-vent compartment fire experiments were conducted [3] to establish the correlation for the mixing at the quasi-steady state. The fuel supply rate was controlled and the measurements include the oxygen concentration vertical profiles, gas temperature, smoke layer heights, and neutral plane height. From the steady-state conservation of oxygen, the mixing ratio, $\dot{m}_e/\dot{m}_o$, can be estimated from the measured oxygen concentration in the lower and upper layer as $\dot{m}_e/\dot{m}_o = \left(Y_{ox,o} - Y_{ox,l}\right)/Y_{ox,l} - Y_{ox,u}$. From the experiments, we found that the mixing ratio is well correlated with Eq. [5] and a linear relationship up to an apparent asymptote for the mixing ratio of 1.28. This can be put into an expression for the mixing ratio as follows:

$$\begin{aligned} \dot{m}_e/\dot{m}_o &= 1.14 \cdot \Psi \quad \text{for } \Psi < 1.1 \\ \dot{m}_e/\dot{m}_o &= 1.28 \qquad \text{for } \Psi \geq 1.1 \end{aligned} \qquad [6]$$

where Ψ represents the right hand side of the Eq. [5]. A well-mixed condition in the compartment fire is defined when the layer interface or the smoke is close to the floor. The opening geometry and fire size plays an important role on the location of the layer interface [3]. When this condition prevails, the properties of the gas in the compartment are said to be uniform and a single zone model can be effectively used to predict the gas temperature and species in the compartment. Nevertheless, in reality a sharp gradient of the oxygen concentration still exists near the floor. In other words, the oxygen that is feeding the flame is not the same as in the bulk smoke layer even though the smoke layer is close to the floor. In order to overcome this, the mixing can be used as a mechanism to help defining the local oxygen feeding the flame in a single zone model. We choose to use a constant maximum value of 1.28 for the mixing ratio as suggested for the well-mixed compartment fires with a single-wall-vent configuration. This limit would apply when the layer is close to the floor.

SINGLE-ZONE MODEL

To create a complex model that could provide an absolute prediction on every aspect of the compartment fire behavior may not be possible at this time. Nevertheless, a simple, yet beneficial model could be derived in order to demonstrate the important mechanisms. Assuming uniform property, we have conservation relationships as:

Mass: $$\rho_o T_o V \frac{d}{dt}\left(1/T\right) + \dot{m} - \dot{m}_o - \dot{m}_F = 0 \qquad [7]$$

Oxygen: $$\rho_o T_o V \frac{d}{dt}\left(Y_{ox}/T\right) + \dot{m}Y_{ox} - \dot{m}_o Y_{ox,o} = -\dot{Q}/\Delta h_{ox} \qquad [8]$$

Energy: $$\frac{V}{\gamma - 1}\frac{dP}{dt} + c_p \dot{m} T - c_p \dot{m}_o T_o - c_p \dot{m}_F T_F = \dot{Q} - \dot{q}_{wall} - \dot{q}_{vent} \qquad [9]$$

Here $\dot{m}$ is the outflow rate, $\dot{m}_o$ is the inflow rate, $\dot{m}_F$ is the fuel mass loss rate, Δh_{ox} is the heat of combustion per unit mass of oxygen, *V* is the enclosure volume, $\dot{q}_{wall}$ is the heat transfer to the boundaries, and $\dot{q}_{vent}$ is the heat loss through the opening via radiation, and $\gamma = c_p / c_v$. Subscript "$_o$" represents ambient condition. By letting the neutral plane be the reference level, mass flow through the vent between the height ($z_a < z < z_b$) is given as:

Vent flow: $$\dot{m}_i = \frac{2}{3} \mathrm{C_d} W_o \sqrt{2g\rho_i(\rho_o - \rho)}\left(z_b^{3/2} - z_a^{3/2}\right) \quad [10]$$

where z_a and z_b are measured from the reference height. The convection heat transfer from gas to the wall is simply:

$$\dot{q}_{conv} = h_c A_w (T - T_{w,0}) \quad [11]$$

where $T_{w,0}$ is the wall surface temperature, A_w is the wall total surface area, and h_c is the convective heat transfer coefficient taken from an empirical correlation developed in a recent scale modeling study for compartment heat transfer by Veloo [15]. This correlation is consistent with Tanaka and Yamada [16] and is developed for a higher range of temperature. It is given as:

$$\frac{h_c}{\rho_o c_p (gl)^{1/2}} = \begin{cases} 3.5\times10^{-3} & ;\theta < 2.2 \\ 16\times10^{-3}\theta - 31.7\times10^{-3} & ;\theta \geq 2.2 \end{cases} \quad [12]$$

where l is the compartment height and $\theta = (T - T_o)/T_o$. Assuming a grey uniform-temperature wall, the radiation exchange between gas and the compartment wall is [2]:

$$\dot{q}_{rad} = \frac{A_w \sigma\left(T^4 - T_{w,0}^4\right)}{1/\varepsilon_g + 1/\varepsilon_w - 1}. \quad [13]$$

As for the heat conduction through the boundary, by spatially discretizing a transient one-dimensional heat equation with the centered difference scheme into n elements, we have a system of algebraic ordinary differential equations as follows:

$$\begin{pmatrix} \frac{dT_{w,1}}{dt} = \frac{k_{w,2}\left(T_{w,2} - T_{w,1}\right) - k_{w,1}\left(T_{w,1} - T_{w,0}\right)}{\Delta x^2 \rho_w c_{pw,1}} \\ \frac{dT_{w,2}}{dt} = \frac{k_{w,3}\left(T_{w,3} - T_{w,2}\right) - k_{w,2}\left(T_{w,2} - T_{w,1}\right)}{\Delta x^2 \rho_w c_{pw,2}} \\ \vdots \\ \frac{dT_{w,n}}{dt} = \frac{k_{w,n+1}\left(T_{w,n+1} - T_{w,n}\right) - k_{w,n}\left(T_{w,n} - T_{w,n-1}\right)}{\Delta x^2 \rho_w c_{pw,n}} \end{pmatrix} \quad [14]$$

Boundary conditions:

$$\frac{-k_{w,1}\left(T_{w,1} - T_{w,0}\right)}{2\Delta x} = h_c\left(T - T_{w,0}\right) + \varepsilon_g \sigma\left(T^4 - T_{w,0}^4\right)$$

$$\frac{-k_{w,n}\left(T_{w,n+1} - T_{w,n-1}\right)}{2\Delta x} = h_{c,ambient}\left(T_{w,n} - T_o\right)$$

A flame extinction condition can be defined by a flammability line that is based on a critical flame temperature below which the extinction occurs and no energy is generated into the system. The flame temperature T_f is given as [17]:

$$c_p\left(T_f - T_l\right) = \frac{\Delta h_c - L + c_p\left(T_v - T_l\right) + \frac{\dot{q}''_{Ext,b}}{\dot{m}_b}}{1 + \left(r/Y_{ox,l}\right)} \quad [15]$$

where *r* is the stoichiometric oxygen to fuel ratio given by, $Y_{ox,l}$ and T_l and are the local oxygen level and temperature of the gas that is feeding the flame respectively. Based upon the extinction flame temperature, the criteria for energy release rate (or burning rate) given in Eq. [1] is expressed as:

$$\dot{m}_b = \begin{cases} \dot{m}_F & ; \quad Y_{ox} > 0 \text{ and } T_f > 1300^\circ\text{C} \\ \dfrac{\dot{m}_o Y_{ox,o}}{r} & ; \quad Y_{ox} = 0 \text{ and } T_f > 1300^\circ\text{C} \\ 0 & ; \quad T_f \le 1300^\circ\text{C} \end{cases} \qquad [16]$$

where $\dot{m}_F$ is given in Eq. [3]. Lastly from the mixing ratio, $\dot{m}_e/\dot{m}_o$ =1.28, described in Section 3, $Y_{ox,l}$ and T_l can be calculated as $Y_{ox,l} = \dfrac{Y_{ox,o} + (\dot{m}_e/\dot{m}_o)Y_{ox,u}}{1+(\dot{m}_e/\dot{m}_o)}$ and $T_l = \dfrac{T_o + (\dot{m}_e/\dot{m}_o)T_u}{1+(\dot{m}_e/\dot{m}_o)}$ respectively.

COMPARTMENT FIRE EXPERIMENT AND MODEL APPLICATION

A series of experiments using a small-scale compartment was conducted in which the quantity and configuration of the fuel were varied under natural ventilation condition of various doorway and window widths. The compartment was built with 2.54 cm (1 inch) thick Type-M Kaowool board. The compartment inner size was measured 40 cm × 40 cm × 120 cm (height × width × depth). Two kinds of the single-wall-vent, doorway-like and window-like, were used. The vent height and the sill height were designed such that they represented the common doorway and widow height in real buildings. The measurements are comprised of fuel mass loss rate, gas temperatures, oxygen concentrations, heat flux to wall surface, and differential pressure near vent. Fig. 1 shows the section view of the compartment and the measurement layout.

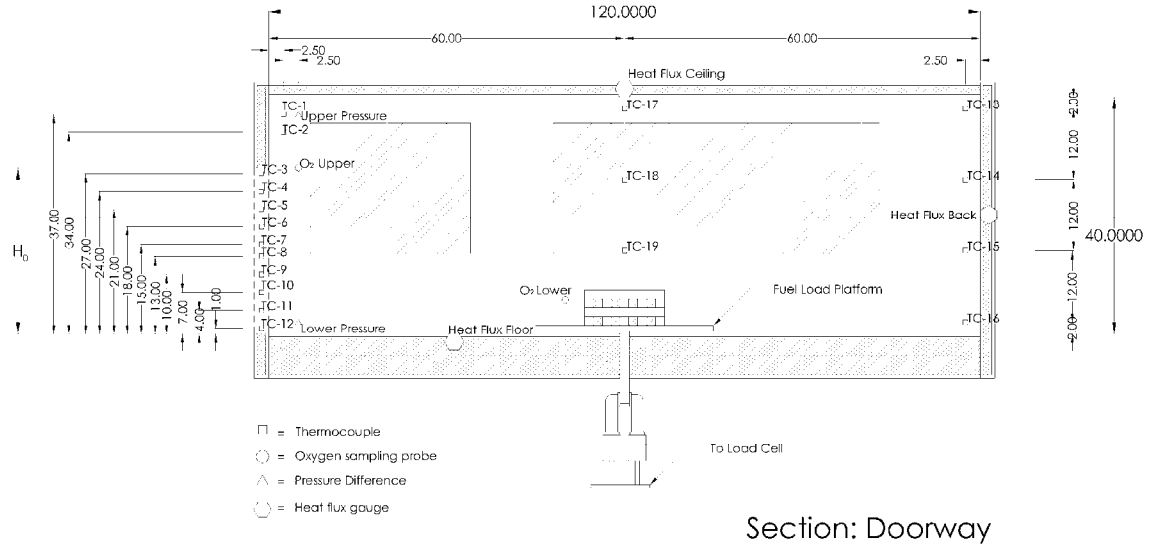

FIGURE 1. Schematic of the compartment and measurement layout

The fuel configurations selected here were the *crib* fire and the *pool* fire. Two types of wood, Oak and Pine, were selected as the material for the crib fire. The crib configurations were designed to have surface controlled burning. Heptane (C7H16) was used for the pool fire tests. Descriptions for wood crib and pool size are presented in Table 1. Table 2 provides the experimental conditions.

TABLE 1. Wood crib and heptane pool description

Crib	b (m)	n_i	n_j	L_i (m)	L_j (m)	N	Type	Pool	Diameter (m)	Heptane volume (ml)
1	0.012	4	7	0.3	0.15	5	Pine	1	7x0.138, 3x0.147	90 (each pan)
2	0.01905	4	4	0.15	0.15	5	Pine	2	0.245	300
3	0.012	5	5	0.15	0.15	4	Pine			
4	0.011	9	9	0.25	0.25	5	Oak			
5	0.022	5	9	0.414	0.207	3	Oak			

TABLE 2. Experimental condition

Test	H_o (m)	W_o (m)	S (m)	A_F	Test	H_o (m)	W_o (m)	S (m)	A_F
Crib1D28x15	0.28	0.15	0.00	0.234	Crib3D28x30	0.28	0.30	0.00	0.119
Crib1W14x20	0.14	0.20	0.14	0.234	Crib3D28x40	0.28	0.40	0.00	0.119
Crib1W14x32	0.14	0.32	0.14	0.234	Crib3W14x32	0.14	0.32	0.14	0.119
Crib2D28x05	0.28	0.05	0.00	0.185	Crib4D28x15	0.28	0.15	0.00	0.403
Crib2D28x15	0.28	0.15	0.00	0.185	Crib5D28x15	0.28	0.15	0.00	0.414
Crib2D28x30	0.28	0.30	0.00	0.185	Pool1D28x15	0.28	0.15	0.00	0.1557
Crib2D28x40	0.28	0.40	0.00	0.185	Pool2D28x15	0.28	0.15	0.00	0.0472
Crib2W14x06	0.14	0.06	0.14	0.185	Pool2D28x30	0.28	0.30	0.00	0.0472
Crib2W14x32	0.14	0.32	0.14	0.185					

Experimental results and the single zone model prediction are presented here for an example case. Fig. 2 shows the transient results for Crib2 with 28 cm high x 30 cm wide opening with the global equivalence ratio of 0.45. The prediction shows good agreement with the measured fuel mass loss rate and the gas temperature.

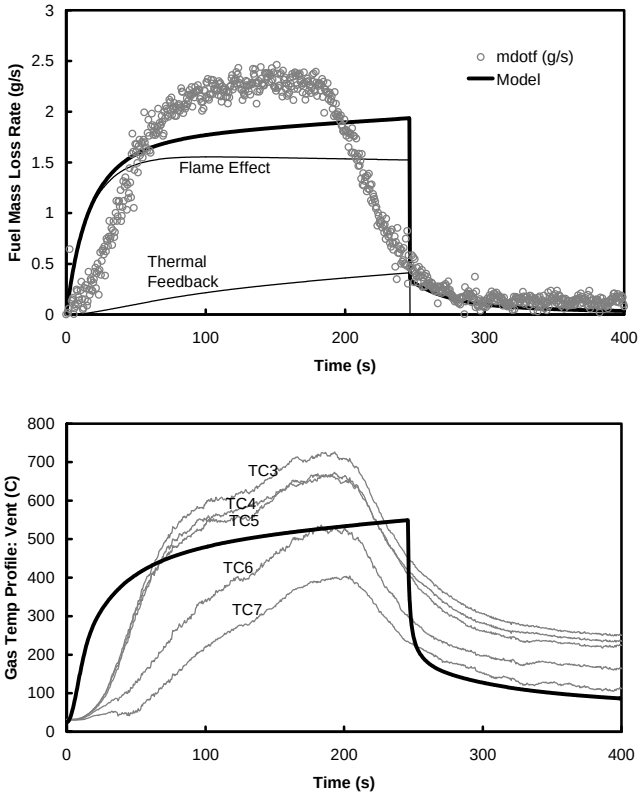

FIGURE 2. Transient results – experiment and single-zone model prediction for Crib 2 with 28 cm x 30 cm opening, GER = 0.45

Burning behaviors can be categorized into 3 cases based on the observed behavior and the global equivalence ratio. The 3 cases are:

Case 1: Steady well-ventilated burning. This is the case where vent is large and the global equivalence ratio is less than one. The flame stabilized above the fuel, and the oxygen in the upper layer is above zero.

Case 2: Steady under-ventilated burning. This case the opening size is reduced and the global equivalence ratio is less than one. The burning is ventilation-limited and the fire area shrinkage occurs. Oxygen in the upper layer is at or near zero. The oscillating flame may take place if the extinction criterion, depending on the local temperature and oxygen, is reached. But the oscillation is only a transient stage for this case and the flame eventually reaches the steady stage where no oscillation occurs and become under-ventilated.

Case 3: Unsteady under-ventilated burning. In this case the opening size is the smallest among all cases. Periodic oscillating flame is observed. The global equivalence ratio is less than one; however, the oxygen in the upper layer is above zero. In this case the extinction criterion is reached and the oscillating flame occurs until the fuel is exhausted. Throughout the burning, the flame does not consume all the oxygen available

In order to present the experiment results and the model prediction in a global perspective, an average peak value was determined for the fuel mass loss rate and the upper layer gas temperature. The average peak value for both measured and predicted variables was determined in the following manner. The time interval corresponding to the fuel mass changing from 80 to 30 percent of its initial mass was identified. All variables were then numerically averaged over this time interval to yield the average peak values. Fig. 3 presents the average peak value of the fuel mass loss rate in terms of the effect of the ventilation ($A_o\sqrt{H_o}\rho_o\sqrt{g}/A_F$) and the wall heat loss (A_s/A_F) [18]. The average peak temperatures are also presented in the same manner in Fig. 4.

The free burning rate is also presented on the right-vertical axis for each crib in Fig. 3. The trend predicted by the model generally agrees well with the experiment for both wood crib and heptane fires. The regimes of burning (case 1 to case 3) based on the observation in the simulation are illustrated on the plot using the horizontal arrow-head line. The number marked on each regime corresponds to the case 1 to case 3 and the abbreviation “Ext” designates the complete flame extinction. As shown by the experiments and simulations on the figure, the burning behavior regime of the heptane pool and wood crib fire do not coincide with each other. For instance, at the same ventilation factor ($A_o\sqrt{H_o}\rho_o\sqrt{g}/A_F$) of 1000 g/m^{2}s, the pool fire is already in its ventilation-limited range while the crib fire is still in the well-ventilation regime. The prediction of the crib shows that in the well-ventilated regime (case 1), the thermal feedback enhancement does not exhibit a strong effect on the mass loss rate and the flame (or oxygen) effect is more dominant as seen by the less value of the crib mass loss rate than its free burning rate. This is also consistent with the experimental result. In addition, no trend is observed for the area ratio, A_s/A_F , in the well-ventilated regime because the thermal effect is small and the crib mainly burns according to its free burning. In other words, for non-porosity-controlled cribs, the stick size is responsible for the mass loss rate of the different crib configuration in the well-ventilated regime. In the under-ventilated regime (case 2 and 3), a general observation from the model and the experiment is that the mass loss rate decreases as the ventilation decreases. However, the wood crib burning dependence on A_s/A_F becomes clearer from the simulation as the burning is now controlled by the air inflow, oxygen reduction in the lower layer and higher gas temperatures as the amount of fuel (A_F) is increased. Hence, without the scale differences, for ventilation-limited fires, the smaller the ratio A_s/A_F , the higher the mass loss rate.

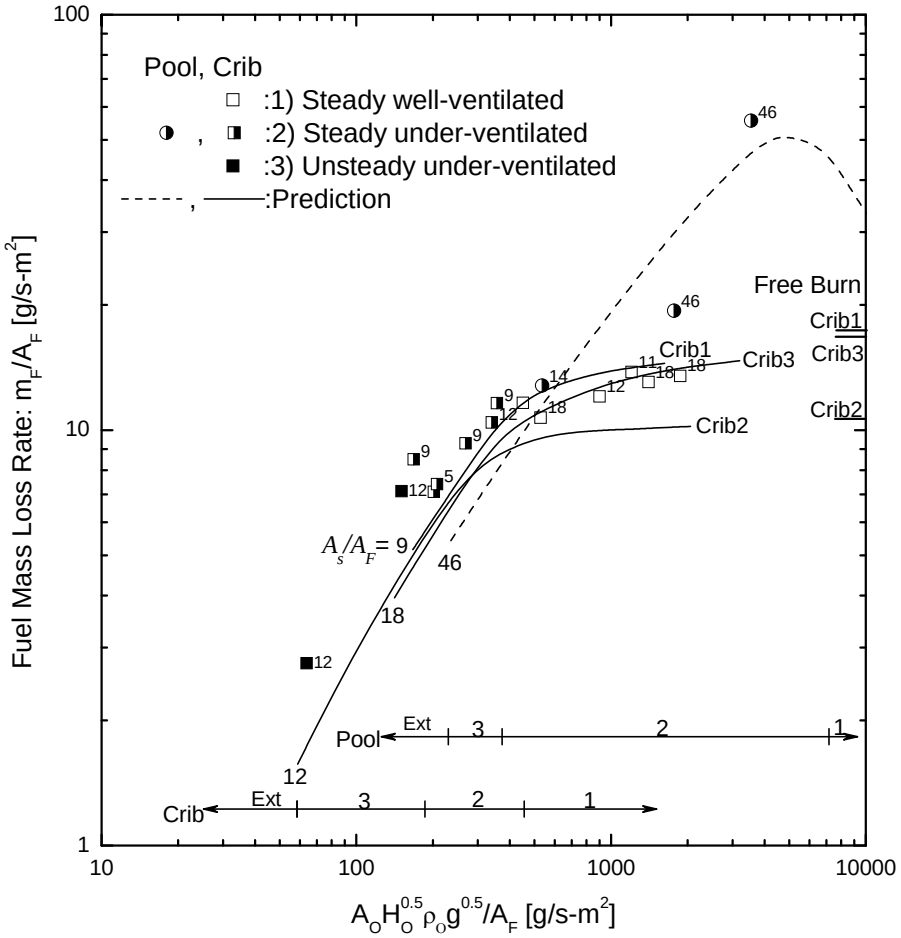

FIGURE 3. Dependence of the peak average fuel mass loss rate on ventilation and wall heat loss

The simulation from the single-zone model is used to investigate the effect of the scale on the burning. The compartment used in the large-scale simulation is geometrically scaled up 4 times from the compartment size used in the experiment. This gives a compartment height of 1.6 m. Crib 2 and Pool 1 are also scaled up similarly to preserve the A_s / A_F ratio. Note that the number of the sticks and layers of the crib does not change; only the stick length and thickness increase by 4. The mass of the fuel is consistent with the increased volume. The results are presented in Fig. 4. The experimental data from Crib 2 and Pool 1 are also included. On each prediction line, the marked number signifies the boundary of the burning regime. For instance, "2 | 1" indicates the boundary between case 1 and case 2 (the steady well-ventilated and the under-ventilated regime). Note that the free burning rate per unit area of the large scale crib is less than the small scale crib because of the larger thickness (*b*), while the free burning rate per unit area of the large pool fire is larger then the small-scale one. The simulation shows for the small-scale pool that at the near ventilation limited (moving Case 1 to Case 2) the thermal effect is dominating as evident from the increase of the mass loss rate to a higher than its free burning value. In the large-scale pool case the thermal effect is less significant. This is reasonable because the larger-scale heptane pool fire has a higher flame emissivity than the small-scale ($\varepsilon_{f,pool}$ = 0.68 vs. 0.22); hence, the external heat feedback is "blocked" more by the sootier large-scale flame. However, the wood crib fires exhibit an opposite behavior. In the small-scale crib, at the near ventilation limited, the oxygen effect is more dominated while in the large-scale crib the mass loss is enhanced more by the thermal feedback. This could be due to the nature of the heptane pool flame that is much sootier than the wood crib fire. In other words, the emissivities of both large-scale and small-scale wood crib are generally small ($\varepsilon_{f,\text{wood crib}}$ = 0.18 vs. 0.05); the higher thermal feedback in

the large-scale case can penetrate through the wood crib flame and enhance the burning more than the small-scale case. In the ventilation limited regime (Case 2 and Case 3) the large-scale configuration shows a higher mass loss rate in both wood crib and the heptane pool fire. Moreover, the flame oscillation in the large-scale simulation seems to take place at a lower ventilation condition than that in the small-scale. The flame extinction regime of the large-scale is also changed to a lower ventilation condition.

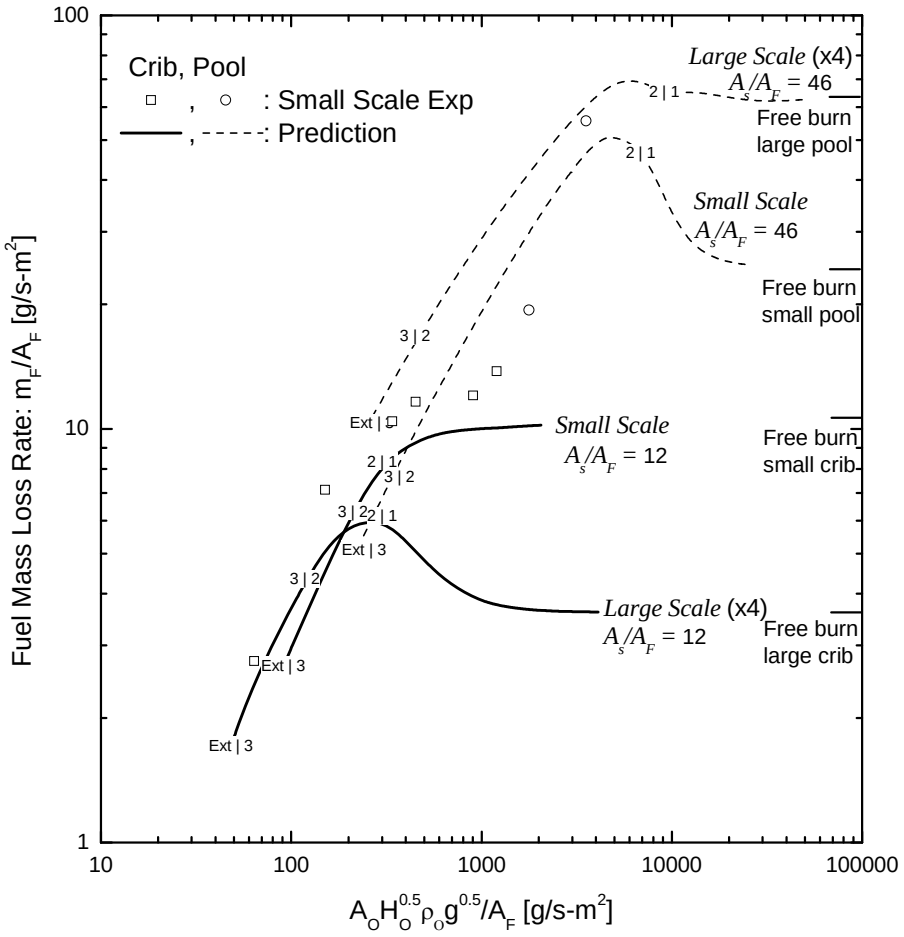

FIGURE 4. Scale and fuel type effects on the compartment fuel mass loss rate

Fig. 5 shows the peak average gas temperature from experiment and the simulation with the ventilation factor. The peak average values in the experiment are determined for both temperatures measured at the vent and near the back wall. The upper end of the error bar represents the peak average value of the vent temperature and the lower end for the back wall. The plot between each end signifies the space average temperature from these two locations. The trend mapped by the simulation follows the experiment data reasonably well. The highest temperature from the simulation for both wood crib and heptane pool fire is found to be at the boundary of well-ventilated and under-ventilated regime, or at the point where the global equivalence ratio is unity. The effect of the wall heat loss to the temperature is quite obvious that the gas temperature increases as the ratio A_s / A_F decreases.

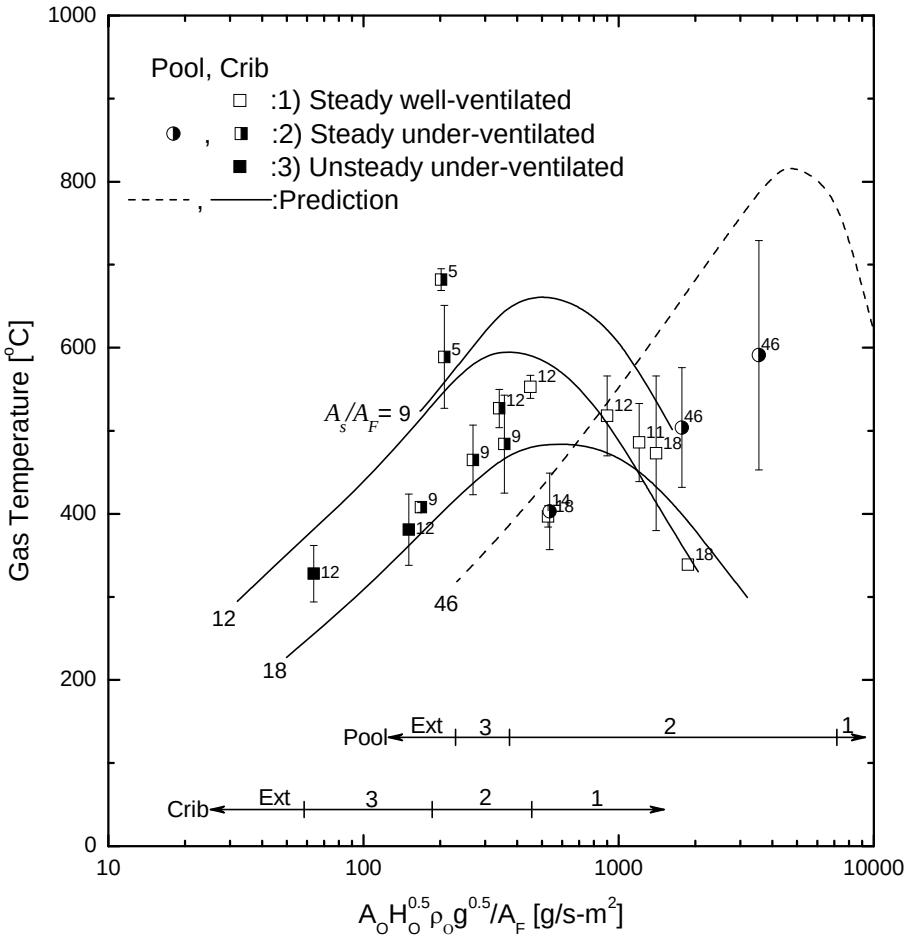

FIGURE 5. Dependence of the peak average gas temperature on ventilation and wall heat loss

The scale effect on the gas temperature is presented in Fig. 6. For the liquid pool fire, the temperature predicted in the large-scale is higher than the small-scale throughout the range of the ventilation. As for the wood crib the large-scale only shows higher temperature than the small-scale in the ventilation limited regime. The temperature from the large-scale simulation exceeds the small-scale temperature at the boundary of the well-ventilated to under-ventilated regime; this confirms a strong thermal feedback from the hot gas layer to the fuel mass loss rate increasing significantly at this location as described in Fig. 4. Note that the temperature presented here is the average peak temperature, which does not represent the maximum temperature recorded in the experiments and the simulations. The maximum peak temperature measured from the largest wood crib experiment in our study is found to be at 890 ºC and the prediction for this test yield a maximum temperature of 840 ºC.

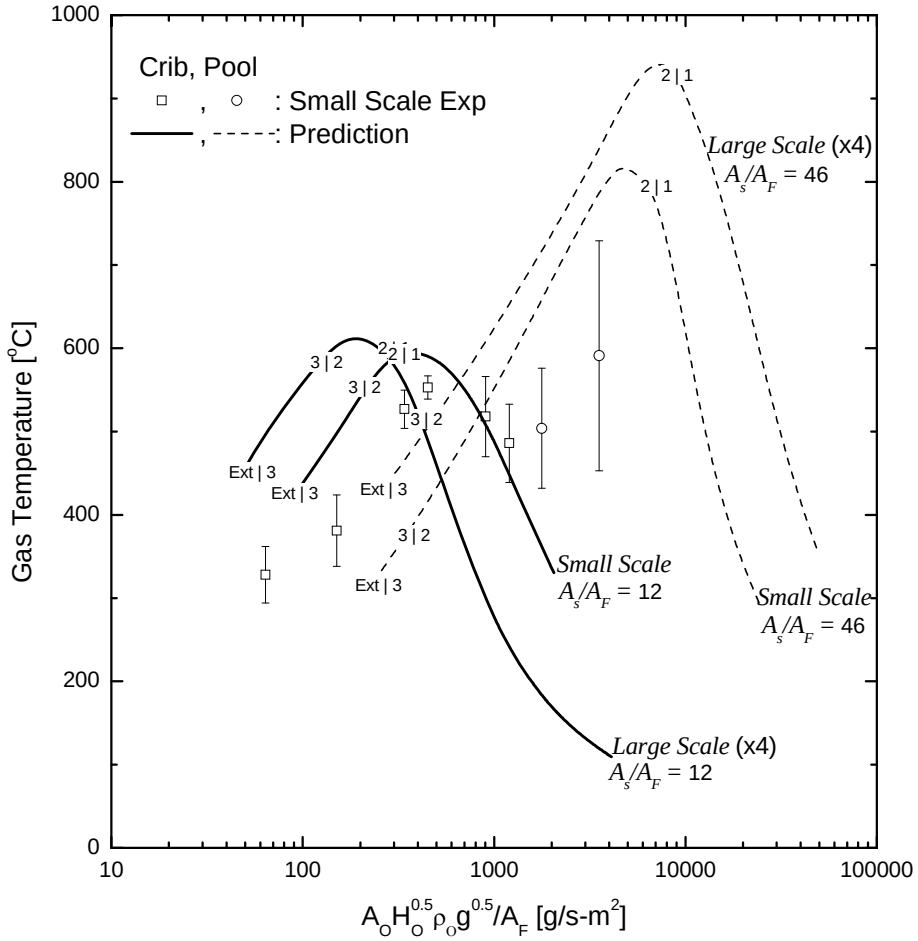

FIGURE 6. Scale and fuel type effects on the compartment fuel mass loss rate

CONCLUDING REMARKS

A single-zone fully-developed compartment fire model that accounts for the fuel type and configuration has been established. The model is capable of predicting the gas temperature and the fuel mass loss rate that can relate to the burn time in a fire for any fuel, scale and ventilation. The model shows good agreement with the experiment and is able to reveal the full range of phenomena associated with fully developed fires as observed in the experiment: response of fuel to thermal and oxygen effects, oscillation, and extinction. Fuel type, scale, ventilation, and heat loss effects have been demonstrated with the model simulations and the experiments. Generally, the higher temperature and mass loss rate are achieved with the bigger scale and the lower ratio of A_s / A_F. The maximum temperature and mass loss rate is achieved when $\phi \approx 1$. The scale effect on the flame emissivity of the heptane pool fires is more than that of the wood crib fires.

ACKNOWLEDGMENTS

This study was supported by the National Institute of Standards and Technology and the John L. Bryan Chair Fund.

REFERENCES

1. Quintiere, J.G., Principles of Fire Behavior, New York: Delmar publishers, 1998.
2. Karlsson, B. and Quintiere, J.G., Enclosure Fire Dynamics, Florida: CRS Press, 1999.
3. Utiskul, Y., "Theoretical and Experimental Study on Fully-Developed Compartment Fires", in Fire Protection Engineering and Mechanical Engineering, University of Maryland: College Park, MD, 2006.
4. Tewarson, A., Lee, J.L., and Pion, R.F. "The Influence of Oxygen Concentration on Fuel Parameters for Fire Modeling", Symp Int Combust 18th. Waterloo, Ont, USA: Combustion Institute, 1981.
5. Santo, G. and Delichatsios, M.A., "Effects of Vitiated Air on Radiation and Completeness of Combustion in Propane Pool Fires", FMRC J.I. 0F0N4.BU, Factory Mutual Research, 1982.
6. Babrauskas, V., "Estimating Large Pool Fire Burning Rates", Fire Technology, 19, 251, 1983.
7. Heskestad, G. "Modeling of Enclosure Fires", Symp Int Combust 14th. PA, USA: The Combustion Institute, 1972.
8. Block, J.A. "A Theoretical can Experimental Study of Nonpropagating Free-Buring Fires". 13th Symposium (International) on Combustion, Salt Lake City, Utah: Combustion Institute, 1970.
9. Quintiere, J.G., "Compartment Fire Modeling", in SFPE Handbook of Fire Protection Engineering, National Fire Protection Association. pp. 3.125 - 3.133, 1995.
10. Quintiere, J.G., McCaffrey, B.J. and Rinkinen, W., "Visualization of Room Fire Induced Smoke Movement and Flow in a Corridor", Fire and Materials, 2:1, 18-24, 1978.
11. McCaffrey, B.J., and Quintiere, J. G., "Buoyancy-Driven Counter-current Flows Generated by a Fire Source", Heat Transfer and Turbulent Buoyant Convection, 2, 457-472, 1977.
12. Zukoski, E.E., "Experimental Study of Environment and Heat Transfer in a Room Fire", NBS Grant No. G8-9014, California Institute of Technology, 1978.
13. Lim, C.S., Zukoski, E. E. and Kubota, T., "Mixing in Doorway Flows and Entrainment in Fire Flames", NBS Grant No. NB82NADA3033, California Institute of Technology, 1984.
14. Quintiere, J.G. and McCaffrey, B.J., "The Burning of Wood and Plastic Cribs in an Enclosure: Volume I", NBSIR 80-2054, National Bureau of Standards, 1980.
15. Veloo, P., "Scale Modeling of the Transient Behavior of Heat Flux in Enclosure Fires", in Fire Protection Engineering, University of Maryland: College Park. p. 127, 2006.
16. Tanaka, T. and Yamada, S., "Reduced Scale Experiments for Convective Heat Transfer in the Early Stage of Fires", International Journal on Engineering Performanced-based Fire Codes. 1:3, 196-203, 1999.
17. Quintiere, J.G. and Rangwala, A.S., "A Theory of Flame Extinction Based on Flame Temperature", Fire and Materials, 28, 387-402, 2003.
18. Y. Utiskul, J.G. Quintiere, A.S. Rangwala, B.A. Ringwelski, K. Wakatsuki and T. Naruse, "Compartment Fire Phenomena under Limited Ventilation". Fire Safety Journal, 40:4, 367-390, 2005.